Exp Brain Res (2017) 235:3833–3841
DOI 10.1007/s00221-017-5101-6

RESEARCH ARTICLE

# Resting GABA concentration predicts inhibitory control during an auditory Go-Nogo task

**Chia-Hsiung Cheng**[1,2,3,4] · **David M. Niddam**[5,6] · **Shih-Chieh Hsu**[4,7] · **Chia-Yih Liu**[4,7] · **Shang-Yueh Tsai**[8,9]

Received: 19 February 2017 / Accepted: 3 October 2017 / Published online: 9 October 2017


**Abstract** Inhibitory control plays an important role in goal-directed behavior. Although substantial inter-individual variability exists in the behavioral performance of response inhibition, the corresponding modulating neurochemical and neurophysiological mechanisms remain unclear. Thus, the present study aimed to explore the relationship between behavioral response inhibition, GABA+ concentrations and automatic sensory gating (SG) in the auditory cortices. We recruited 19 healthy adults to undergo magnetoencephalography, magnetic resonance spectroscopy (MRS), and behavioral experiments. A paired-stimulus paradigm was used to study SG of the auditory cortices, and an auditory-driven Go-Nogo task was used to evaluate the behavioral response inhibition. Resting GABA+ concentrations were measured in the bilateral superior temporal gyri by means of MRS. Neither GABA+ concentrations nor auditory SG showed significant hemispheric asymmetry. However, an enhanced SG (lower ratio) was found to correlate with improved behavioral inhibition. Moreover, a higher GABA+ concentration was strongly related to improved inhibitory control. These findings highlight the important role of automatic neurophysiological processes and inhibitory neurotransmitters in the prediction of the behavioral performance of inhibitory control.

**Keywords** Response inhibition · M100 · Sensory gating · Magnetic resonance spectroscopy (MRS) · Magnetoencephalography (MEG)

## Introduction

Inhibitory control plays a pivotal role in successful performance of goal-directed tasks in daily life. Inhibitory control relies on both bottom-up and top-down brain mechanisms. From a bottom-up perspective, our brains automatically inhibit, or filter out, irrelevant sensory information to

**Electronic supplementary material** The online version of this article (doi:10.1007/s00221-017-5101-6) contains supplementary material, which is available to authorized users.

✉ Chia-Hsiung Cheng
ch.cheng@mail.cgu.edu.tw; chiahsiung.cheng@gmail.com

✉ Shang-Yueh Tsai
sytsai@nccu.edu.tw

[1] Department of Occupational Therapy and Graduate Institute of Behavioral Sciences, Chang Gung University, No. 259, Wenhua 1st Rd, Taoyuan 333, Taiwan

[2] Laboratory of Brain Imaging and Neural Dynamics (BIND Lab), Chang Gung University, Taoyuan, Taiwan

[3] Healthy Aging Research Center, Chang Gung University, Taoyuan, Taiwan

[4] Department of Psychiatry, Chang Gung Memorial Hospital, Linkou, Taiwan

[5] Institute of Brain Science, National Yang-Ming University, Taipei, Taiwan

[6] Brain Research Center, National Yang-Ming University, Taipei, Taiwan

[7] School of Medicine, Chang Gung University, Taoyuan, Taiwan

[8] Graduate Institute of Applied Physics, National Chengchi University, No. 64, Sec.2, ZhiNan Rd, Taipei 116, Taiwan

[9] Mind, Brain and Learning Center, National Chengchi University, Taipei, Taiwan

prevent flooding of higher-hierarchical centers, e.g., frontal regions (Chao and Knight 1997; Cheng et al. 2012; Cheng and Lin 2013). This type of automatic inhibitory function in the cortex has been extensively studied using sensory gating (SG)—a phenomenon of attenuated neural activity to the second identical stimulus in a paired-stimulus paradigm (Clementz et al. 1998; Boutros and Belger 1999; Karl et al. 2006). In scenarios where careful decision-making or action execution is required, inappropriate responses may selectively be inhibited through top-down control. Successful execution of a goal-directed task in a distractible environment requires not only the task-relevant information to be enhanced but also concurrent inhibition of task-irrelevant information. The Go-Nogo task is an experimental paradigm tailored to study this type of attentive response inhibition (Hester et al. 2004; Kenemans et al. 2005).

Several lines of evidence support the notion that perceptual function, e.g., pre-attentive SG, is associated with cognition, e.g., memory or attentive response inhibition. For example, a better SG ability has been shown to correlate with a lower commission error rate and better discriminability in the Delay Memory Task (Lijffijt et al. 2009). Furthermore, a significant association between SG ability and explicit memory function, as measured by the Verbal Paired Associate Task, was found in patients with schizophrenia (Hsieh et al. 2004). Moreover, SG deficits in patients with schizophrenia were ameliorated by cognitive training with emphasis on auditory discrimination and verbal memory (Popov et al. 2011).

A substantial inter-individual variability exists in automatic SG responses as well as in behavioral performance of response inhibition. However, the underlying modulating mechanisms of this variability remain unclear. In the visual cortex, the concentration of γ-Aminobutyric acid (GABA), a major inhibitory neurotransmitter in the mammalian brain, has been associated with several types of cognitive function (Edden et al. 2009; Yoon et al. 2010). Thus, individual differences in sensory cortical GABA concentrations may account, at least in part, for this variability.

In the present study, we investigated the relationship between pre-attentive automatic inhibition, attentive inhibitory control and GABA concentrations in the auditory system. More specifically, the auditory SG function was assessed by means of whole-head magnetoencephalography (MEG) combined with an auditory paired-stimulus paradigm and attentive Inhibitory control was assessed with an auditory-driven Go-Nogo task. Furthermore, in vivo resting GABA concentrations in the auditory cortices, i.e., the superior temporal gyri (STG), were obtained by means of non-invasive magnetic resonance spectroscopy (MRS), using spectral editing (Mullins et al. 2014; Puts et al. 2015; Harris et al. 2017a, b). Since SG ratio is defined as the amplitude of the cortical response to the second stimulus divided by the amplitude of the cortical response to the first stimulus, a lower SG ratio indicates enhanced automatic inhibition. Hence, we hypothesized that the auditory SG ratio would be negatively correlated with behavioral performance of inhibitory control and, furthermore, predicted a negative association between the SG ratio and GABA concentration. Finally, we hypothesized that higher GABA baseline concentrations would be related to improved behavioral performance of inhibitory control.

## Materials and methods

### Participants

To exclude the potential effects of gender on SG and GABA concentrations, 19 healthy male adults between the age of 20 and 34 years (mean, $M = 25.79$; standard error of the mean, SEM = 0.79) were recruited in the present study. All subjects were right-handed with a handedness score > 70%, as assessed by the Edinburg Inventory (Oldfield 1971). All subjects self-reported that they and their first-degree relatives were free from major neurological and psychiatric diseases. The Institutional Review Board of Taipei Veterans General Hospital approved the protocol, and informed consent was obtained from each individual.

### MEG recordings and analyses

To study the SG ability, a paired-stimulus paradigm was presented to the subjects with inter-stimulus intervals (ISIs) of 500 ms and inter-pair intervals of 6 s. Auditory stimuli consisted of 800 Hz click-like tones (duration = 20 ms, including 5 m rise and fall times), binaurally delivered through plastic earphones at the intensity of 70 dB above the participants' hearing threshold. These stimuli were made using a sound editing program (GoldWave Digital Audio Editor, GoldWave Inc.), and run by the Presentation software (version 11.3, Neurobehavioral Systems, Inc., Davis, USA).

Auditory evoked fields (AEFs) were recorded with a whole-head 306-channel MEG system (Vectorview, Elekta-Neuromag, Helsinki, Finland). The online bandpass and sampling rate were set at [0.1, 200] Hz and 500 Hz, respectively. Epochs contaminated by prominent electrooculogram (> 300 μV) and MEG artifacts (> 3000 fT/cm) were excluded from averaging. A total of at least 100 artifact-free trials containing matching stimulus pairs of Stimulus 1 (S1) and Stimulus 2 (S2) were averaged for further analyses.

The AEFs were digitally bandpass filtered (1–30 Hz) offline and then baseline corrected (− 100 to 0 ms). The modeling of cortical spatiotemporal dynamics of AEFs was performed using the depth-weighted minimum norm estimate (MNE) as implemented in the Brainstorm software

(Tadel et al. 2011). The representation of folded cortical surfaces was used to resolve the forward problem by means of an overlapping-sphere model, which detects the strength of a set of electric dipoles located at the cortical surface (Huang et al. 1999). Cortically constrained MNE was computed for each subject and each stimulus type (i.e., S1 and S2) with a source space consisting of ~ 15,000 dipoles over the cortex. The MNE source maps of each subject and each stimulus type were then geometrically rescaled to the Montreal Neurological Institute Colin27 brain template using Brainstorm's multilinear registration technique. The time-resolved magnitude of each dipole was normalized to its fluctuations over the baseline, yielding a z-scored map.

Two-source modeling was applied to anatomically constrain source space to the left superior temporal gyrus (LSTG) and right superior temporal gyrus (RSTG). Initially, two regions of interest (ROIs) were identified according to the individual maximal cortical responses around the M100 components in RSTG and LSTG (Cheng et al. 2010; Cheng and Lin 2012; Edgar et al. 2014; Demopoulos et al. 2017). A cluster of ~ 40 cortical vertices corresponding to 5–6 $cm^2$ in both RSTG and LSTG was then manually selected. Finally, absolute z values of S1 and S2 at the peak latency of the M100 component (90–160 ms after the stimulus onset) were extracted for the calculation of SG ratio, defined as S2/S1. A lower ratio indicates a better SG function.

### MRS acquisition and analyses

All imaging data were acquired with a 3T MR system (TRIO, SIEMENS Medical Solutions, Erlangen, Germany) using a 32-channel phased-array head coil. A high-resolution 3D MPRAGE anatomical scan (TR/TE/FA: 2530 ms/3.03 ms/7 degrees; FOV: 256 × 256 × 176; voxel size: 1 × 1 × 1 $mm^3$) was initially obtained for localization of the spectroscopic volumes of interest (VOI). For MRS scans, two VOIs (size: 20 × 25 × 25 $mm^3$) were manually positioned at the bilateral STG. The center of each VOI was placed at the upper surface of the STG with the posterior wall of the VOI just anterior to the parietal-temporal-occipital junction. To further control the quality of the spectra, a pre-scan was carried out using a point resolved spectroscopy (PRESS) sequence (TR/TE = 2000/68 ms, sample points = 2048, bandwidth = 2000 Hz, 16 averages). Spectra were analyzed and displayed online to evaluate the linewidth, water suppression and noise level. A MEGA-PRESS sequence was then used for GABA measurements (Mescher et al. 1998). For each VOI, a total of 300 spectra were acquired using the following parameters: TR/TE = 2000/68 ms, sample points = 2048, bandwidth = 2000 Hz, phase cycling steps = 4. Edit-on and edit-off spectra were acquired in an interleaved fashion. Thus, the 300 spectra were acquired as 75 repeats of a 4-step phase cycle with the editing pulse switched to edit-on and edit-off on alternate phase cycles. GABA-editing was achieved with a 15-ms Gaussian pulse applied at 1.9 ppm for edit-on spectra and at 7.5 ppm for edit-off spectra. In addition, a non-water suppressed (NWS) MRS scan was acquired to obtain an unsuppressed water signal for normalization.

For each subject, on and off steps were saved separately and the first four spectra were excluded. Data processing including phase correction and pairwise frequency alignment based on the creatine (Cr) peak was performed in Matlab (The MathWorks, Natick, USA) using an in-house script (Tsai et al. 2016). The GABA signal at 3.0 ppm was quantified by fitting a two-Gaussian model in the spectral range of 2.79–3.55 ppm with a linear baseline term (Edden et al. 2014). The Glx signal (combination of Glutamate and Glutamine) at 3.75 ppm was quantified by fitting a two-Gaussian model in the spectral range of 3.5–4.0 ppm with a linear baseline term. The Cr peak at 3.0 ppm was fitted by a Lorentzian line shape on edit-off spectra in the spectral range of 2.72–3.12 ppm. The water signal was fitted by a Lorentzian line shape function using the NWS spectra in the spectral range of 3.8–5.6 ppm. The quantified GABA+ (GABA and macromolecules) were normalized to the water signal using the water scaling method and corrected for partial volume and relaxation effects using the following equations (Edden et al. 2012; Puts et al. 2013; Tsai et al. 2016).

$$[\mathrm{GABA+}] = \frac{\mathrm{CSF} + \mathrm{GM} \times 0.78 + \mathrm{WM} \times 0.64}{1 - \mathrm{CSF}} \times [\mathrm{H_2O}] \times \frac{S_{\mathrm{GABA}}}{S_{\mathrm{H_2O}}} \times \frac{\mathrm{ATT}_{\mathrm{H_2O}}}{\mathrm{ATT}_{\mathrm{GABA}}} \times \frac{1}{\mathrm{eff}} \times \mathrm{NH}_{\mathrm{ratio}},$$

$$\mathrm{ATT} = \exp\left(\frac{-\mathrm{TE}}{\mathrm{T2}}\right) \times \left(1 - \exp\left(\frac{-\mathrm{TR}}{\mathrm{T1}}\right)\right),$$

where [GABA+] is the partial volume-corrected GABA concentration determined using water as a reference. $[H_2O]$ is the water concentration of pure water, which is 55.55 M in this case. $s_{GABA}/s_{H_2O}$ is the ratio of quantified GABA+ and water signal by fitting. ATT was used to account for T1 and T2 relaxation effects. The T1 and T2 parameters used are 1.27 and 0.092 s for water, 1.30 and 0.088 s for GABA and 1.25 and 0.2 s for Glx. Eff is the editing efficiency and is 0.5. $HN_{ratio}$ is the ratio of the proton number between metabolite and water. $NH_{ratio}$ is 1 for GABA and 2 for Glx.

The fitting errors of GABA+ and water peak are defined as the standard deviation of the residue divided by peak heights and total fitting errors were defined as the square root of the sum of squares fitting errors of GABA+ and water (Mikkelsen et al. 2016). Data were excluded from the statistical analysis if the total fitting errors were larger than 15% and line widths of Cr over 12 Hz. This resulted in MRS data from 4 LSTGs and 5 RSTGs to be excluded from further analysis. For the quality metrics ($M \pm$ SEM) of the

MRS data, the frequency drift were 3.06 ± 0.68 Hz for the LSTG and 2.44 ± 0.47 Hz for the RSTG. Line widths of Cr and water were 7.17 ± 0.13 Hz and 11.20 ± 0.46 Hz for the LSTG. For the RSTG, line widths of Cr and water were 7.25 ± 0.12 Hz and 11.16 ± 0.32 Hz. The fitting errors of GABA+ were 8.51 ± 0.61% in the LSTG and 7.57 ± 0.38% in the RSTG. The fitting errors of Glx were 6.28 ± 0.51% in the LSTG and 6.19 ± 0.41% in the RSTG. The SNR was calculated using spectra without editing (edit-off). We defined the signal (S) as the area of the fitted Cr peak divided by 2*(linewidth of Cr) and noise (N) was defined as the standard deviation of spectra in the range between 9.5–11 ppm. The resulting SNR (S/N) in the LSTG were 130.1 ± 25.4 and 146.7 ± 18.5 in the RSTG.

### Behavioral Go-Nogo task

The auditory Go-Nogo task was performed after MEG recordings in a separate laboratory. Auditory stimuli were delivered with a 20 ms duration and an intensity of 70 dB above the participants' hearing threshold. The ISI varied between 1.0 and 1.2 s to avoid expectation effects. Participants were instructed to press the button with their right index finger to low-pitch (800 Hz) tones (Go, 80%) as quickly and accurately as possible, and to inhibit responses to infrequent high-pitch (850 Hz) tones (Nogo, 20%). A short practice was given before the formal experiment. Each subject performed two blocks of the auditory Go-Nogo task, with each one consisting of 160 Go trials and 40 Nogo trials.

A better performance of response inhibition was indexed by a higher accuracy rate of Nogo stimuli and was defined as [(trial number of successful inhibition to Nogo stimuli/total number of Nogo stimuli) × 100%].

### Statistical analysis

Statistical analyses were performed with the IBM SPSS (version 19) statistics software. All the data were presented as $M \pm$ SEM. Each parameter was evaluated with a Kolmogorov–Smirnov one-sample test, and the results showed the data to be normally distributed (all $p$ values > 0.05). The hemispheric differences of M100 SG ratio and GABA+ levels were examined by paired $t$ tests. The associations among M100 SG ratios, GABA+ concentrations, and behavioral Nogo accuracy rates were evaluated with Pearson's correlation coefficients. Due to the possible influences of the individual S1 amplitude on the SG ratio value, the S1 amplitude was controlled for when computing the correlation between SG ratio and other parameters, i.e., GABA+ concentration, Nogo accuracy rate. Adjusted $p$ values of 0.05, corrected for multiple comparisons by the Benjamini and Hochberg approach (Benjamini and Hochberg 1995), were used to set the significance level.

## Results

Figure 1a shows the grand-averaged AEFs and the corresponding cortical source maps of M100 components in response to S1 and S2. Figure 1b exhibits the source amplitude as a function of time in the RSTG and LSTG. M100 component is the most prominent deflection of AEFs and was clearly detectable for S1 and S2 in both hemispheres. S2/S1 ratio could, thus, be obtained from each participant. There were no significant differences between LSTG ($M$ = 0.48, SEM = 0.04) and RSTG ($M$ = 0.53, SEM = 0.03) in terms of M100 SG ratio ($t$ = 0.98, $p$ = 0.34).

Figure 2 displays an example of VOI placements and the corresponding GABA+ spectra of LSTG and RSTG. MRS data from 4 LSTGs and 5 RSTGs were excluded from further analysis due to insufficient quality. The spectra (Supplementary Fig. 1) and fitted GABA+ signals (Supplementary Fig. 2) of each individual are displayed in the supplementary file. Again, GABA+ concentrations did not differ significantly ($t$ = 0.49, $p$ = 0.63) between LSTG ($M$ = 10.95, SEM = 0.36) and RSTG ($M$ = 11.01, SEM = 0.42).

Figure 3 displays scatter plots for the three parameters in each hemisphere. We first investigated whether the automatic inhibition ability, as indexed by M100 SG ratio, could predict the level of the behavioral inhibition response. A lower M100 SG ratio was correlated with a higher Nogo accuracy rate in the RSTG ($r$ = − 0.622, adjusted $p$ = 0.009), but not in the LSTG ($r$ = 0.063, adjusted $p$ = 0.439). The results of Fishers $r$-to-$z$ transformation confirmed that the correlation was right-lateralized ($Z$ = 2.2, $p$ = 0.028). We then examined whether the behavioral performance of inhibitory control could be predicted by a more fundamental neurochemical factor. A significant positive association between GABA+ concentration and Nogo accuracy rate was observed in the RSTG ($r$ = 0.547, adjusted $p$ = 0.032), but not in the LSTG ($r$ = 0.222, adjusted $p$ = 0.439) No significant lateralization of correlation was observed ($Z$ = − 0.93, $p$ = 0.35). No correlation was found between M100 SG ratio and GABA+ concentration in each hemisphere. After applying the Fishers $r$-to-$z$ transformation, the correlation coefficient values between left and right hemispheres were not significantly different ($Z$ = 0.35, $p$ = 0.73).

Glx concentrations were also obtained in each VOI and were 7.01 ± 0.27 and 6.34 ± 0.25 in the LSTG and RSTG, respectively. When Glx concentrations entered as a controlling factor in the association analyses, the above results

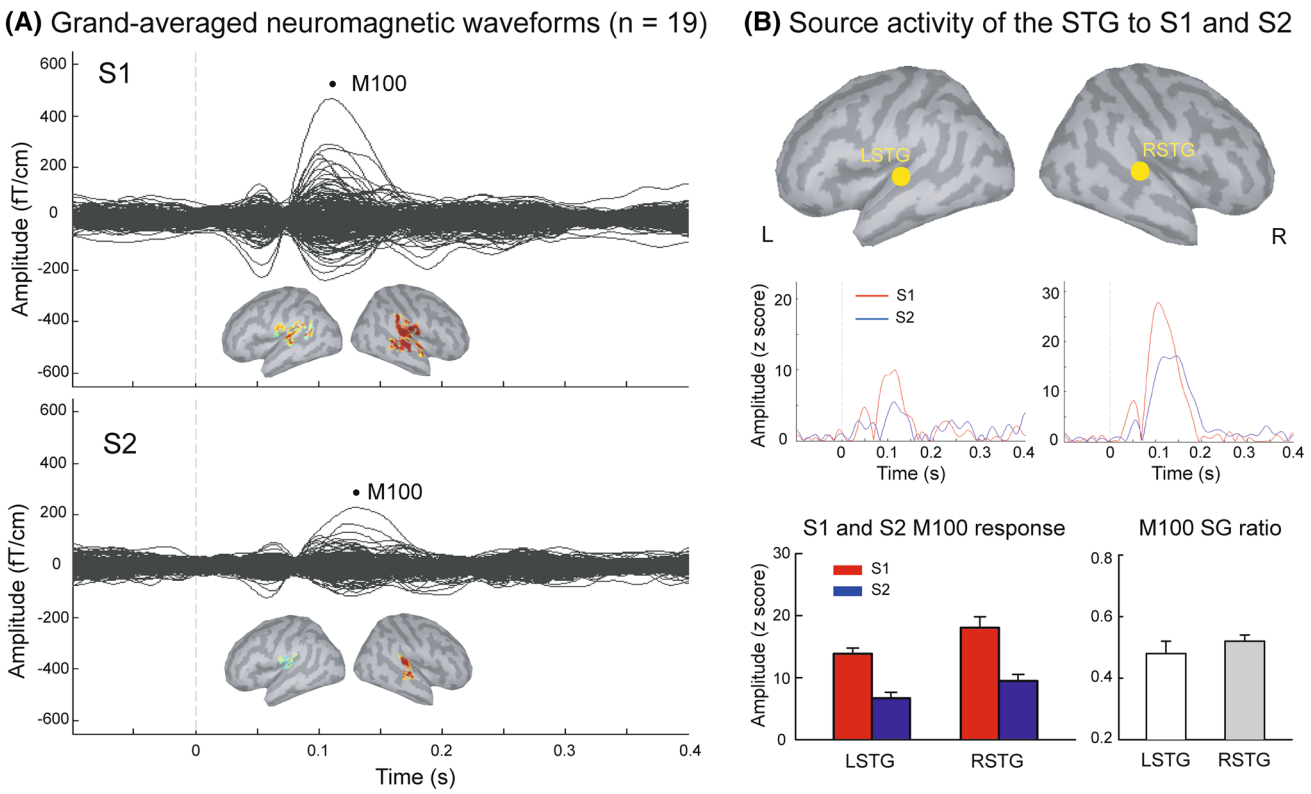


**Fig. 1** **a** Grand-averaged auditory evoked responses and the cortical activation of M100 component to Stimulus 1 (S1) and Stimulus 2 (S2) in the paired-click paradigm. **b** The regions of interest (ROIs) were manually identified in the left superior temporal gyrus (LSTG) and the right superior temporal gyrus (RSTG). The source activities from these two ROIs were extracted from each stimulus type and each individual. The sensory gating (SG) ratio was calculated as S2/S1 of M100 source amplitudes. The M100 SG ratios did not show hemispheric differences

remained either significant or were borderline significant in the RSTG after the correction for multiple comparisons (Supplementary Table).

## Discussion

This study investigated the relationship between pre-attentive automatic inhibition, inhibitory neurotransmitter concentration and attentive inhibitory control in the auditory system. In accord with our hypothesis, we found a negative association between M100 SG and behavioral performance during response inhibition, i.e., better SG with improved response inhibition. Notably, higher baseline concentrations of GABA+ were predictive of better behavioral inhibitory control. All of these associations were only observed in the right hemisphere.

Our study demonstrated a relationship between automatic and attentive inhibitory function. It has been reported that a better P50 gating ability was correlated with fewer commission errors in the Delay Memory Task (Lijffijt et al. 2009). Further on, children with stronger P50 and N100 gating effects had a shorter reaction time using the Go-Nogo paradigm (Liu et al. 2011). However, despite its popularity in clinical research, recent studies suggest the SG ratio based on the P50 to be less reliable than the ratio based on the N100 (Fuerst et al. 2007; Rentzsch et al. 2008). Furthermore, identification of P50 component is relatively subjective and relies more on the researcher's experience. Thus, a more reliable and easily identified component is preferable for the SG calculation. The N100 or M100 is the most robust deflection of AEPs or AEFs and can be easily identified in each individual (Godey et al. 2001; Cheng et al. 2015). As a result, we consider the observed association between pre-attentive M100 SG and behavioral response inhibition as robust and, therefore, having a greater clinical potential.

We also found a significant association between auditory MRS-measured GABA+ concentration and response inhibition performance, as assessed by the auditory-driven Go-Nogo task. A previous study, examining the integration of multisensory stimuli, showed that the auditory GABA concentration was correlated with audiovisual perception (Balz et al. 2016). In the same vein, a higher level of occipital GABA concentration was found to predict a

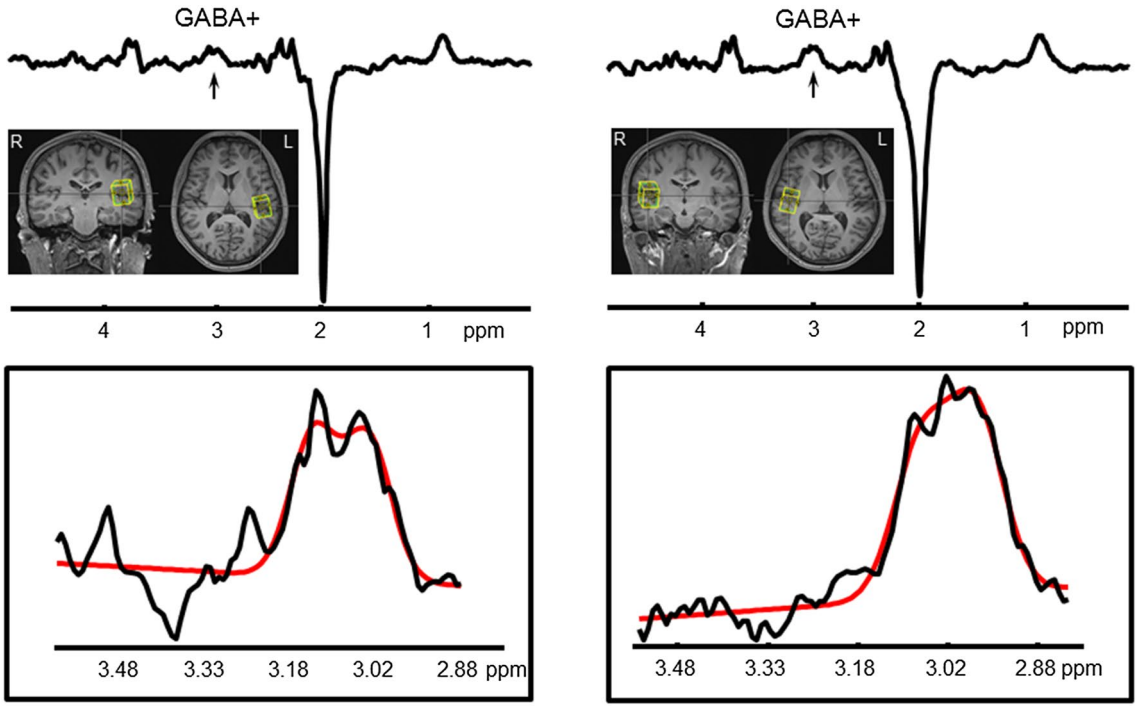


**Fig. 2** Top: edited spectra from the bilateral superior temporal gyrus of a representative subject. The edited spectrum results from the difference between the edit-on and edit-off data. Bottom: fitted peak of GABA+ (Red line) using a two-Gaussian model with 7 variables (2 height, width, frequency, splitting, baseline offset, baseline gradient) in the spectral range of 2.79–3.55 ppm

better performance in a visual orientation discrimination task (Edden et al. 2009). A similar relationship was also observed in the sensorimotor cortex (Puts et al. 2011, 2015). The aforementioned results suggest that sensory cortices, at least in part, contribute to the modality-specific prediction of higher-order perceptual function. This should be considered in context of the major role of the frontal cortex in the modulation of response inhibition (Silveri et al. 2013; Ribeiro et al. 2015). Our study encourages further investigation into the role of other sensory cortices in the processing of inhibitory control using the same modality-matching design (e.g., sensorimotor GABA concentration and somatosensory-driven Go-Nogo task) as the present study.

The association between behavioral inhibitory control and pre-attentive SG was confined to the right hemisphere. Previous studies, along with our results, do not support the presence of hemispheric asymmetry in SG processing (Thoma et al. 2003; Hirano et al. 2010). In the present study, the Go-Nogo task required sustained attention to minimize the error rate. Converging evidence indicates that the attention network is right-lateralized (Yan et al. 2009). It is, therefore, reasonable to find a more significant association between behavioral performance of inhibitory control and SG in the right hemisphere. Our study did also not find a significant hemispheric asymmetry in GABA+ concentration. However, we cannot rule out that the quality of the GABA signal in the LSTG might have contributed to the lack of significance. The LSTG spectrum exhibited a clear shoulder to the left of the GABA+ peak at 3 ppm, which was not seen in the RSTG (Fig. 2). This difference potentially resulted from the inclusion of non-brain tissue (e.g., lipid) or improper editing leading to subtraction artifacts during post-processing.

Evidence points to the involvement of cortical and subcortical circuits in both automatic and attentive inhibitory control. Auditory SG may rely on several cortical regions, including the temporo-parietal and prefrontal cortices, in the early phase, and the hippocampus in the later phase (Grunwald et al. 2003). Furthermore, oscillations and synchronization of thalamocortical activity are modulated via projections from the thalamus to cortical areas (McCormick and Bal 1994). In agreement with the involvement of these circuits, abnormal auditory SG in schizophrenia patients was associated with increased or prolonged hemodynamic responses in the temporal cortex, prefrontal cortex, and thalamus (Tregellas et al. 2007). Behavioral response inhibition has been suggested to rely on a frontostriatal circuit connected with the basal ganglia (Aron 2011). Jahfari and colleagues further proposed that response inhibition was mediated through the pathway from cortical regions (e.g., pre-supplementary area) to the caudate, globus pallidus, and thalamus, while action control was implemented from the

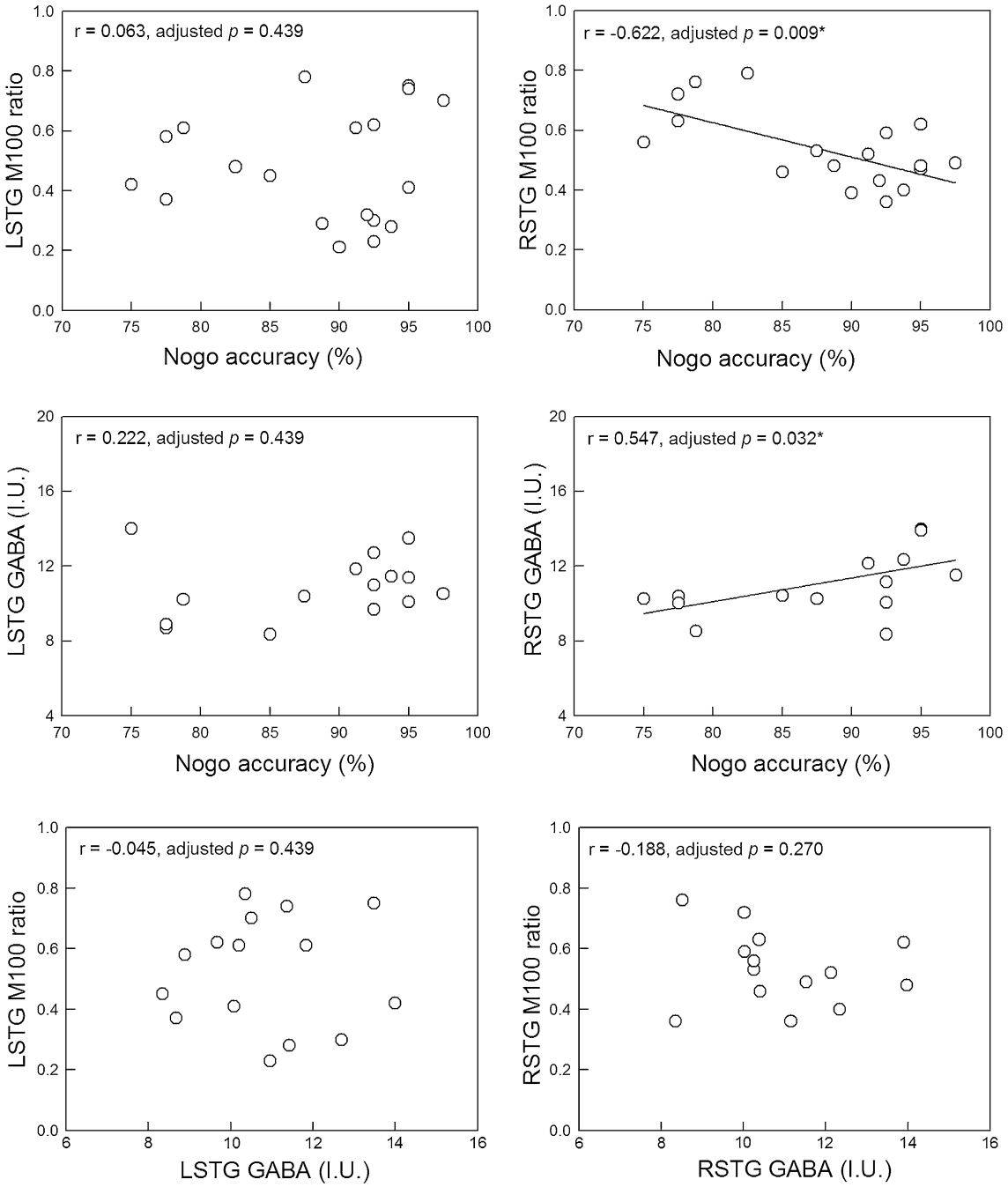


**Fig. 3** Associations among the performance of response inhibition (i.e., Nogo accuracy rate), M100 sensory gating (SG) ratio, and GABA concentration in the left and right superior temporal gyri (LSTG and RSTG, respectively)

thalamus to the primary motor cortex via the thalamocortical pathway (Jahfari et al. 2011).

Several important considerations and limitations of the present study need to be addressed. Firstly, the sample size was relatively small. Nevertheless, we still observed robust associations such as those between GABA+ concentration and behavioral performance of inhibitory control. We consider the present study as an exploratory pilot and invite future studies with larger sample sizes to validate it. Secondly, the cortical response to the Go-Nogo task was not recorded by MEG. In addition to the auditory paired-stimulus paradigm, our participants underwent several blocks of other MEG tasks (data published elsewhere). The completion of these experiments took more than 40 min, and exhausted most of the subjects as reported after the MEG experiment. Accordingly, only the behavioral data of the

Go-Nogo task were collected, during which the subjects could freely move their heads and limbs as long as they continued to focus on the task. Future investigations should focus on the associations among the neural correlates of response inhibition, sensory gating and GABA concentration. Thirdly, in contrast to our expectation, a significant association between M100 SG ratio and GABA+ concentration was not found. A tempting explanation might be that an additional factor moderates the relationship between M100 SG and GABA+ concentration. Finally, regarding the spectral quality, baseline fluctuations and artifacts were observed in the spectra from the STG. Baseline noise may increase the fitting uncertainty. Further on, regions around the STG usually suffer from higher field inhomogeneity compared to regions in the occipital and parietal lobes. This may explain the higher fitting errors in our study (~ 8%) than those previously reported for the occipital lobe (4–5%) (Evans et al. 2013; Harris et al. 2015; Mikkelsen et al. 2016). Another contributing factor may be the smaller VOI (12.5 ml) used to cover the region of interest in the present study. Smaller volumes are associated with poorer signal-to-noise ratio. As a result, more time was spent on repeating shimming procedures in the pre-scan to achieve an acceptable linewidth for subsequent data collection in the STG.

In conclusion, this work not only replicated previous studies showing an association between automatic and attentive inhibitory control, but also demonstrated that the behavioral response inhibition was predicted by resting GABA+ concentration in the right STG. The present study provided empirical evidence for the modulation of inhibitory control through multiple levels, i.e., through a neurotransmitter-neurophysiological-behavioral axis.

**Acknowledgements** This work was supported by Chang Gung Memorial Hospital (CMRPD1E0291, CMRPD1E0292), Chang Gung University (BMRPE25), Healthy Aging Research Center at Chang Gung University (EMRPD1F0321, EMRPD1G0241), and Ministry of Science and Technology (MOST-104-2314-B-182-001-MY2, MOST-105-2628-B-182-004-MY3), Taiwan.

**Compliance with ethical standards**

**Conflicts of interest** The authors declare that they have no conflict of interest.

## References

Aron AR (2011) From reactive to proactive and selective control: developing a richer model for stopping inappropriate responses. Biol Psychiatry 69:e55–e68

Balz J, Keil J, Roa Romero Y, Mekle R, Schubert F, Aydin S, Ittermann B, Gallinat J, Senkowski D (2016) GABA concentration in superior temporal sulcus predicts gamma power and perception in the sound-induced flash illusion. Neuroimage 125:724–730

Benjamini Y, Hochberg Y (1995) Controlling the false discovery rate: a practical and powerful approach to multiple testing. J R Statist Soc B 57:289–330

Boutros NN, Belger A (1999) Midlatency evoked potentials attenuation and augmentation reflect different aspects of sensory gating. Biol Psychiatry 45:917–922

Chao LL, Knight RT (1997) Prefrontal deficits in attention and inhibitory control with aging. Cereb Cortex 7:63–69

Cheng CH, Lin YY (2012) The effects of aging on lifetime of auditory sensory memory in humans. Biol Psychol 89:306–312

Cheng CH, Lin YY (2013) Aging-related decline in somatosensory inhibition of the human cerebral cortex. Exp Brain Res 226:145–152

Cheng CH, Hsu WY, Shih YH, Lin HC, Liao KK, Wu ZA, Lin YY (2010) Differential cerebral reactivity to shortest and longer tones: neuromagnetic and behavioral evidence. Hear Res 268:260–270

Cheng CH, Wang PN, Hsu WY, Lin YY (2012) Inadequate inhibition of redundant auditory inputs in Alzheimer's disease: an MEG study. Biol Psychol 89:365–373

Cheng CH, Baillet S, Lin YY (2015) Region-specific reduction of auditory sensory gating in older adults. Brain Cogn 101:64–72

Clementz BA, Geyer MA, Braff DL (1998) Poor P50 suppression among schizophrenia patients and their first-degree biological relatives. Am J Psychiatry 155:1691–1694

Demopoulos C, Yu N, Tripp J, Mota N, Brandes-Aitken AN, Desai SS, Hill SS, Antovich AD, Harris J, Honma S, Mizuiri D, Nagarajan SS, Marco EJ (2017) Magnetoencephalographic imaging of auditory and somatosensory cortical responses in children with autism and sensory processing dysfunction. Front Hum Neurosci 11:259

Edden RA, Muthukumaraswamy SD, Freeman TC, Singh KD (2009) Orientation discrimination performance is predicted by GABA concentration and gamma oscillation frequency in human primary visual cortex. J Neurosci 29:15721–15726

Edden RA, Intrapiromkul J, Zhu H, Cheng Y, Barker PB (2012) Measuring T2 in vivo with J-difference editing: application to GABA at 3 Tesla. J Magn Reson Imaging 35:229–234

Edden RA, Puts NA, Harris AD, Barker PB, Evans CJ (2014) Gannet: a batch-processing tool for the quantitative analysis of gamma-aminobutyric acid-edited MR spectroscopy spectra. J Magn Reson Imaging 40:1445–1452

Edgar JC, Lanza MR, Daina AB, Monroe JF, Khan SY, Blaskey L, Cannon KM, Jenkins J 3rd, Qasmieh S, Levy SE, Roberts TP (2014) Missing and delayed auditory responses in young and older children with autism spectrum disorders. Front Hum Neurosci 8:417

Evans CJ, Puts NA, Robson SE, Boy F, McGonigle DJ, Sumner P, Singh KD, Edden RA (2013) Subtraction artifacts and frequency (mis-)alignment in J-difference GABA editing. J Magn Reson Imaging 38:970–975

Fuerst DR, Gallinat J, Boutros NN (2007) Range of sensory gating values and test-retest reliability in normal subjects. Psychophysiology 44:620–626

Godey B, Schwartz D, de Graaf JB, Chauvel P, Liegeois-Chauvel C (2001) Neuromagnetic source localization of auditory evoked fields and intracerebral evoked potentials: a comparison of data in the same patients. Clin Neurophysiol 112:1850–1859

Grunwald T, Boutros NN, Pezer N, von Oertzen J, Fernandez G, Schaller C, Elger CE (2003) Neuronal substrates of sensory gating within the human brain. Biol Psychiatry 53:511–519

Harris AD, Puts NA, Barker PB, Edden RA (2015) Spectral-editing measurements of GABA in the human brain with and without macromolecule suppression. Magn Reson Med 74:1523–1529

Harris AD, Puts NAJ, Wijtenburg SA, Rowland LM, Mikkelsen M, Barker PB, Evans CJ, Edden RAE (2017a) Normalizing data from GABA-edited MEGA-PRESS implementations at 3 Tesla. Magn Reson Imaging 42:8–15

Harris AD, Saleh MG, Edden RA (2017b) Edited 1 H magnetic resonance spectroscopy in vivo: methods and metabolites. Magn Reson Med 77:1377–1389

Hester R, Fassbender C, Garavan H (2004) Individual differences in error processing: a review and reanalysis of three event-related fMRI studies using the GO/NOGO task. Cereb Cortex 14:986–994

Hirano Y, Hirano S, Maekawa T, Obayashi C, Oribe N, Monji A, Kasai K, Kanba S, Onitsuka T (2010) Auditory gating deficit to human voices in schizophrenia: a MEG study. Schizophr Res 117:61–67

Hsieh MH, Liu K, Liu SK, Chiu MJ, Hwu HG, Chen AC (2004) Memory impairment and auditory evoked potential gating deficit in schizophrenia. Psychiatry Res 130:161–169

Huang MX, Mosher JC, Leahy RM (1999) A sensor-weighted overlapping-sphere head model and exhaustive head model comparison for MEG. Phys Med Biol 44:423–440

Jahfari S, Waldorp L, van den Wildenberg WP, Scholte HS, Ridderinkhof KR, Forstmann BU (2011) Effective connectivity reveals important roles for both the hyperdirect (fronto-subthalamic) and the indirect (fronto-striatal-pallidal) fronto-basal ganglia pathways during response inhibition. J Neurosci 31:6891–6899

Karl A, Malta LS, Maercker A (2006) Meta-analytic review of event-related potential studies in post-traumatic stress disorder. Biol Psychol 71:123–147

Kenemans JL, Bekker EM, Lijffijt M, Overtoom CC, Jonkman LM, Verbaten MN (2005) Attention deficit and impulsivity: selecting, shifting, and stopping. Int J Psychophysiol 58:59–70

Lijffijt M, Lane SD, Meier SL, Boutros NN, Burroughs S, Steinberg JL, Moeller FG, Swann AC (2009) P50, N100, and P200 sensory gating: relationships with behavioral inhibition, attention, and working memory. Psychophysiology 46:1059–1068

Liu T, Xiao T, Shi J, Zhao L (2011) Sensory gating, inhibition control and child intelligence: an event-related potentials study. Neuroscience 189:250–257

McCormick DA, Bal T (1994) Sensory gating mechanisms of the thalamus. Curr Opin Neurobiol 4:550–556

Mescher M, Merkle H, Kirsch J, Garwood M, Gruetter R (1998) Simultaneous in vivo spectral editing and water suppression. NMR Biomed 11:266–272

Mikkelsen M, Singh KD, Sumner P, Evans CJ (2016) Comparison of the repeatability of GABA-edited magnetic resonance spectroscopy with and without macromolecule suppression. Magn Reson Med 75:946–953

Mullins PG, McGonigle DJ, O'Gorman RL, Puts NA, Vidyasagar R, Evans CJ, Edden RA (2014) Current practice in the use of MEGA-PRESS spectroscopy for the detection of GABA. Neuroimage 86:43–52

Oldfield RC (1971) The assessment and analysis of handedness: the Edinburgh inventory. Neuropsychologia 9:97–113

Popov T, Jordanov T, Rockstroh B, Elbert T, Merzenich MM, Miller GA (2011) Specific cognitive training normalizes auditory sensory gating in schizophrenia: a randomized trial. Biol Psychiatry 69:465–471

Puts NA, Edden RA, Evans CJ, McGlone F, McGonigle DJ (2011) Regionally specific human GABA concentration correlates with tactile discrimination thresholds. J Neurosci 31:16556–16560

Puts NA, Barker PB, Edden RA (2013) Measuring the longitudinal relaxation time of GABA in vivo at 3 Tesla. J Magn Reson Imaging 37:999–1003

Puts NA, Harris AD, Crocetti D, Nettles C, Singer HS, Tommerdahl M, Edden RA, Mostofsky SH (2015) Reduced GABAergic inhibition and abnormal sensory symptoms in children with Tourette syndrome. J Neurophysiol 114:808–817

Rentzsch J, Jockers-Scherubl MC, Boutros NN, Gallinat J (2008) Test-retest reliability of P50, N100 and P200 auditory sensory gating in healthy subjects. Int J Psychophysiol 67:81–90

Ribeiro MJ, Violante IR, Bernardino I, Edden RA, Castelo-Branco M (2015) Abnormal relationship between GABA, neurophysiology and impulsive behavior in neurofibromatosis type 1. Cortex 64:194–208

Silveri MM, Sneider JT, Crowley DJ, Covell MJ, Acharya D, Rosso IM, Jensen JE (2013) Frontal lobe gamma-aminobutyric acid levels during adolescence: associations with impulsivity and response inhibition. Biol Psychiatry 74:296–304

Tadel F, Baillet S, Mosher JC, Pantazis D, Leahy RM (2011) Brainstorm: a user-friendly application for MEG/EEG analysis. Comput Intell Neurosci 2011:879716

Thoma RJ, Hanlon FM, Moses SN, Edgar JC, Huang M, Weisend MP, Irwin J, Sherwood A, Paulson K, Bustillo J, Adler LE, Miller GA, Canive JM (2003) Lateralization of auditory sensory gating and neuropsychological dysfunction in schizophrenia. Am J Psychiatry 160:1595–1605

Tregellas JR, Davalos DB, Rojas DC, Waldo MC, Gibson L, Wylie K, Du YP, Freedman R (2007) Increased hemodynamic response in the hippocampus, thalamus and prefrontal cortex during abnormal sensory gating in schizophrenia. Schizophr Res 92:262–272

Tsai SY, Fang CH, Wu TY, Lin YR (2016) Effects of frequency drift on the quantification of gamma-aminobutyric acid using MEGA-PRESS. Sci Rep 6:24564

Yan H, Zuo XN, Wang D, Wang J, Zhu C, Milham MP, Zhang D, Zang Y (2009) Hemispheric asymmetry in cognitive division of anterior cingulate cortex: a resting-state functional connectivity study. Neuroimage 47:1579–1589

Yoon JH, Maddock RJ, Rokem A, Silver MA, Minzenberg MJ, Ragland JD, Carter CS (2010) GABA concentration is reduced in visual cortex in schizophrenia and correlates with orientation-specific surround suppression. J Neurosci 30:3777–3781